HEAVY NUCLEUS COLLISIONS BETWEEN 20 AND 60 GeV/NUCLEON.

The JACEE Collaboration

T.H.Burnett[h], S.Dake[b], M.Fuki[b], J.C.Gregory[g], T.Hayashi[d], R.Holynski[i], J.Iwai[h], W.V.Jones[e], A.Jurak[i], J.J.Lord[h], O.Miyamura[c], T.Ogata[a], T.A.Parnell[f], T.Saito[a], T.Tabuki[a], Y.Takahashi[g], T.Tominaga[c], B.Wilczynska[i], R.J.Wilkes[h], W.Wolter[i], B.Wosiek[i].

a) ICR, University of Tokyo; b) Kobe University;
c) Osaka University; d) Waseda University;
e) Louisiana State University;
f) Marshall Space Flight Center;
g) University of Alabama in Huntsville;
h) University of Washington;
i) Institute of Nuclear Physics, 30-055 Kraków, Poland.

1. Introduction

Interest in studying ralativistic nucleus-nucleus interactions arises from the fact that they offer an opportunity to probe nuclear matter at high density and temperature. It is expected that under such extreme conditions a transition from hadronic matter into quark-gluon plasma occurs and that in the interactions of highly relativistic nuclei such conditions are created [1]. Before energetic nuclei beams will be available at new ion accelerators, cosmic rays remain a unique source of high energy heavy nuclei. JACEE-3 experiment was designed for study the collisions of heavy cosmic ray nuclei with different nuclear targets at energies beyond 20 GeV/nucleon.

2. Experimental method

JACCE-3 experiment was carried out using a combined electronic counters and an emulsion chamber detector, which was exposed to the cosmic rays on a balloon at an altitude of 5 g/cm^2. The electronic counters were placed on the top of a 50 x 50 cm^2 emulsion chamber. The counter system measures the energies (between 20 and 60 GeV/nucleon), charges (from Z=6) and determines trajectories of incident nuclei. It registers also the burst energies released in the interactions. The emulsion chamber serves simultaneously as both target and coordinate/ionization recorder. Details of the apparatus are given in [2].

The charges of projectile fragments and emission angles of all charged secondaries were measured in consecutive layers of emulsion and/or CR-39 plates downstream the interaction vertex. Charged particles in the forward cone were detected in the emulsion chamber without ambiguity. For each event the following multiplicities were determined:

N_F- number of multicharged projectile fragments $(Z \geq 2)$;

N_p- number of released protons from incident nucleus,

$N_p = Z_p - \sum_{i=1}^{N_F} Z_{F,i}$, where Z_p is the charge of primary nucleus;

N_{sf}- number of relativistic $(\beta \geq 0.7)$ singly charged secondaries emitted in the forward hemisphere: $\theta \leq \theta_{1/2}$, where $\theta_{1/2}$ corresponds to $\pi/2$ in the center of mass of proton-proton collision;

$N_{mf} = N_{sf} - N_p$, number of produced charged particles (mesons);

N_{sp}-number of spectator protons (see explanation below);

$N_{part} = N_p - N_{sp}$, number of protons participating in the collision.

Spectator nucleons are not involved in the collision. The number of spectator protons, N_{sp}, can be determined for each event by selecting from singly charged particles those fulfiling a given emission angle criteria [3]. Among participated nucleons $(N_{part} A_p/Z_p)$ are wounded nucleons which interact inelasticaly in the target and nucleons which do not contribute to the particle production but still participate in the collision as the secondaries scatter off them. It is not possible to distinguish experimentally between wounded protons and those originating from cascade processes, however it is natural to assume that N_{part} is related to the number of wounded protons.

3. Results

The analysis was performed on an unbiased sample of heavy primary $(Z_p \geq 22)$ interactions with three different targets: light target=CHO, emulsion and lead. The detailed measurements have been completed for 70 interactions with $E_p \leq 60$ GeV/n out of 120 heavy nuclei recorded. Table 1 summarizes the inclusive data for interactions of "iron" group nuclei on different targets. Multiplicities and dispersions are calculated for the forward cone only. The values of the $\bar{N}_{mf}/D$ ratio are close to 1 independently of the target mass being consistent with the predictions of the superposition models for nucleus-nucleus interactions [4]. In Figs.1a,b,c the inclusive pseudorapidity distributions obtained on different targets are presented. The increased of the particle production on heavier targets in forward region is seen. In Table 2 we compare our results with the data for proton collisions with the same targets [5]. The p-nucleus data are taken in the same angular region and are extrapolated to the same primary energy $\langle E_p \rangle$. The ratio of the average multiplicity in nucleus-nucleus collisions to the mean multiplicity in p-nucleus interactions can be compared to the average number of wounded nucleons in projectile nucleus $\bar{N}_{wn}$, calculated from the simple geometrical formula: $\bar{N}_{wn} = A_p \sigma_{pA_T} / \sigma_{A_p A_T}$. Within the limits of statistical errors these two quantities agree with each other. Thus, we observe an extension of p-nucleus data to nucleus-nucleus ones on the base of simple superposition of independent collisions of nucleons from projectile nucleus.

If we select the events with different number of wounded nucleons than, we expect (basing on a superposition picture) that the multiplicity in nucleus-nucleus collisions will depend linearly on the number of wounded nucleons. Experimentally it is only possible to do a selection according to the number of participating nucleons, so the quantitative comparison with model predictions is not possible. Qualitatively we observe the increase of the multiplicity with increasing number of participating nucleons (Fig.2), but this dependence is much weaker than the one expected from superposition of p-nucleus collisions. This discrepancy may be explained by the fact that among N_{part} there are protons which do not contribute efficiently to the particle production. On the other hand we do not expect a dependence of $\bar{N}_{mf}$ on the number of spectator nucleons, unless the latter are not correlated with participating nucleons. Only for events with a total disintegration of primary nucleus into singly charged fragments such correlation exists. In Fig.3 the dependence of $\bar{N}_{mf}$ on the number of spectator nucleons is shown.

From the central rapidity densities we can estimate the energy density created in the collision. Using the formula given by Bjorken [1] and taking $\bar{P}_{\perp}$=0.4 GeV/c we obtain mean energy densities smaller than 0.5 GeV/fm^3. This is below the critical value required for the phase transition [1]. For the highest multiplicity events the energy density approaches 1 GeV/fm^3. The characteristics of these events will be presented separately at this conference.

4. Conclusions

The presented results from JACEE-3 experiment (multiplicities, $\bar{N}$/D ratios, comparison with p-nucleus data) support the hypothesis that nucleus-nucleus interactions can be considered as a simple superposition of independent p-nucleus collisions. The similar conclusion was obtained from an analysis of ^{22}Ne-emulsion interactions at primary momentum 4.1 A GeV/c and with a high event statistics [6]. No evident signals of phase transition have been observed, suggesting that the detection of exotic phenomena requires a high statistics experiments with a possibility to look for specific signatures.

References

1. See for example: E.Shuryak, Phys.Rep. 61,71(1980), J.D.Bjorken Phys.Rev.D27,140 (1983), J.Cleymans et al., Z.Phys.C17,341(83).
2. JACEE Collaboration, 18th ICRC Conf.Papers 9,375,379 (1983).
3. A.S.Goldhaber, Phys.Lett.B53,306 (1974).
4. A.Bialas etal., Nucl.Phys.B111,461 (1976), K.Kinoshita et al., Z.Phys.C8,205 (1981), A.Capella et al., preprint TH.3700-CERN.
5. W.Busza et al., Phys.Rev.D22,13 (1980).

6.B.Wosiek et al.,this conference paper HE1.4-7.

Table 1.

A_T TARGET MASS	No. of events	$\langle Z_p \rangle$	$\langle E_p \rangle_{GeV/n}$	$\bar{N}_{mf}$	$\bar{N}_{mt}/D$
CHO	45	25.1	36	21.9± 3.0	1.09±.19
Emulsion	10	25.0	28	28.9±11.4	.80±.36
Pb	15	24.8	34	41.1±10.6	1.00±.32

Table 2.

A_T	$\bar{N}_m^{FeA_T}(\eta^{LAB} \geq 2)$	$\bar{N}_m^{pA_T}(\eta^{LAB} \geq 2)$	$\bar{N}_m^{FeA_T}/\bar{N}_m^{pA_T}$	$\bar{N}_{wn}^{Fe}(A_T)^{calc.}$
CHO	22.8 ± 3.3	2.6±0.2	8.8±1.4	6.6
Em	29.8±11.6	3.0±0.3	9.9±4.0	10.3
Pb	45.5±12.3	3.0±0.45	15.2±4.7	18.3

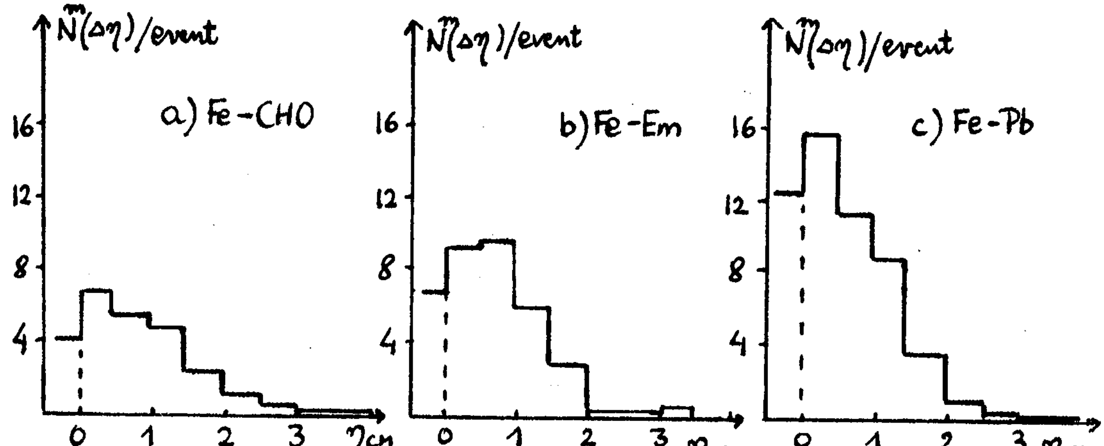

Figure 1.

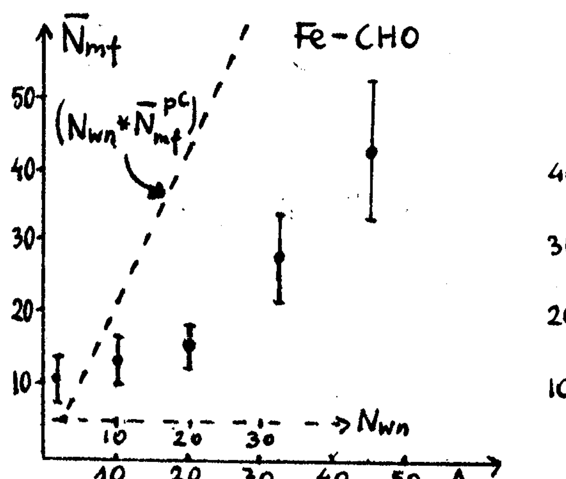

Figure 2.

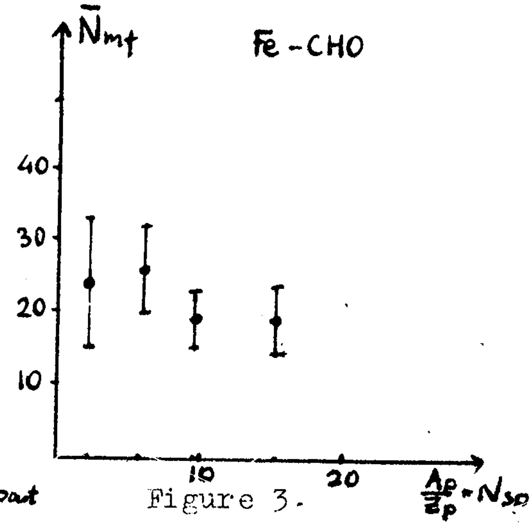

Figure 3.